RSC Advances

PAPER

View Article Online
View Journal | View Issue

Cite this: *RSC Adv.*, 2014, **4**, 13172

Metal-free organic dyes containing thiadiazole unit for dye-sensitized solar cells: a combined experimental and theoretical study†

Gangala Siva Kumar,[ab] Kola Srinivas,[ab] Balaiah Shanigaram,[b] Dyaga Bharath,[a] Surya Prakash Singh,*[be] K. Bhanuprakash,*[b] V. Jayathirtha Rao,*[ace] Ashraful Islam[d] and Liyuan Han[d]

Received 5th December 2013
Accepted 24th February 2014

DOI: 10.1039/c3ra47330a

www.rsc.org/advances

We have designed and synthesized four new metal free D–A–π–A type dyes (**9–12**) with variations in their acceptor/anchor groups. The four dyes carry *tert*-butyl substituted triphenylamine as donor, thiadiazole as acceptor and bithiophene as π-spacer. Cyanoacetic acid, rhodanine-3-acetic acid, 2-(4-methoxyphenyl)-acetic acid and 2-phenylacetic acid are used as acceptor/anchor groups, respectively in the dyes **9–12**. The acceptor/anchor effect on their photophysical, electrochemical and photovoltaic properties was investigated. The dyes exhibited good power conversion efficiency ranging from 1.95–4.12%. Among the four dyes, **9** showed the best photovoltaic performance: short-circuit current density (J_{sc}) of 8.50 mA cm^{-2}, open-circuit voltage (V_{oc}) of 645 mV and fill factor (FF) of 0.75, corresponding to an overall conversion efficiency of 4.12% under standard global AM 1.5 solar light conditions.

Introduction

Due to the increasing global energy demands and decline of natural energy resources, much attention has been focused by researchers to harness solar energy in recent years. Among several solar energy technologies, dye-sensitized solar cells have attracted immense attention owing to their energy conversion, low production cost compared to the conventional inorganic Si-based solar cells.[1] To date, over 11% efficiency has been reported for the DSSCs with Ru based complexes as dyes.[2] Metal free organic dyes have received much attention because of their high molar extinction co-efficient, synthetic flexibility, low cost and compliance with environmental issues. Several metal free organic dyes have been reported with the efficiency ranging from 5–10.3%.[3,4] Metal free organic dyes with D–π–A architecture[5] are promising due to their long range absorption, ease in tuning their photo-physical, electrochemical and photovoltaic properties by varying donor, π-bridge and acceptor moieties. Various entities like triphenylamine,[6–8] carbazole,[9] indoline,[10,11] coumarin,[12,13] fluorene,[14–16] and phenothiazine,[17] are used as donor motifs. Moieties like methine,[18] benzene,[19,20] and thiophene[21] are employed as π-spacers and electron deficient groups like cyanoacetic acid[5,22,23] or rhodanine-3-acetic acid[24] acts as acceptor/anchor.

Metal free organic dyes with molecular architecture D–A–π–A, containing an additional acceptor group compared to the dyes with D–π–A architecture have been recently reported.[25] The additional acceptor acts as an electron trap and facilitates electron transfer from donor to the end group acceptor/anchor. The D–A–π–A dyes have advantages like improved photo and thermal stability, high open circuit voltage and red-shifted absorption.[26] Several electron withdrawing groups such as benzothiadiazole,[27–29] benzotriazole,[30,31] quinoxaline,[32] diketopyrrolopyrrole,[33,34] thienopyrazine,[35] thiazole,[36] and bithiazole,[37] have been used as additional acceptor units. The DSSCs with D–A–π–A dyes have exhibited ~9% power conversion efficiency, under AM 1.5 G irradiation.[38]

As a part of our research efforts[39–42] to study the dependence of photovoltaic performance of DSSC on structural modifications of organic dyes, herein we report the synthesis of four new D–A–π–A type dyes (**9–12**; Scheme 1) with variations in the acceptor/anchor groups. Their photophysical, electrochemical and photovoltaic properties are also explored. The four dyes consist of *tert*-butyl substituted triphenylamine as donor, thiadiazole as acceptor and bithiophene as π-spacer. Cyanoacetic acid, rhodanine-3-acetic acid, 2-(4-methoxyphenyl)acetic acid and 2-phenylacetic acid are used as acceptor/anchor groups, respectively in the dyes **9–12**. The *tert*-butyl groups on triphenylamine hinder the intermolecular aggregation. To the best of

[a]*Crop Protection Chemicals Division, Uppal Road Tarnaka, Hyderabad 500007, India. E-mail: jrao@iict.res.in*

[b]*Inorganic and Physical Chemistry Division, Uppal Road Tarnaka, Hyderabad 500007, India*

[c]*Academy of Scientific & Innovative Research-IICT, CSIR-Indian Institute of Chemical Technology, Uppal Road Tarnaka, Hyderabad 500007, India*

[d]*Photovoltaic Materials Unit, National Institute for Materials Science, 1-2-1 Sengen, Tsukuba, Ibaraki 305-0047, Japan*

[e]*National Institute for Solar Energy, New Delhi, India*

† Electronic supplementary information (ESI) available: Absorption, fluorescence and computational details of dyes **9–12**. See DOI: 10.1039/c3ra47330a

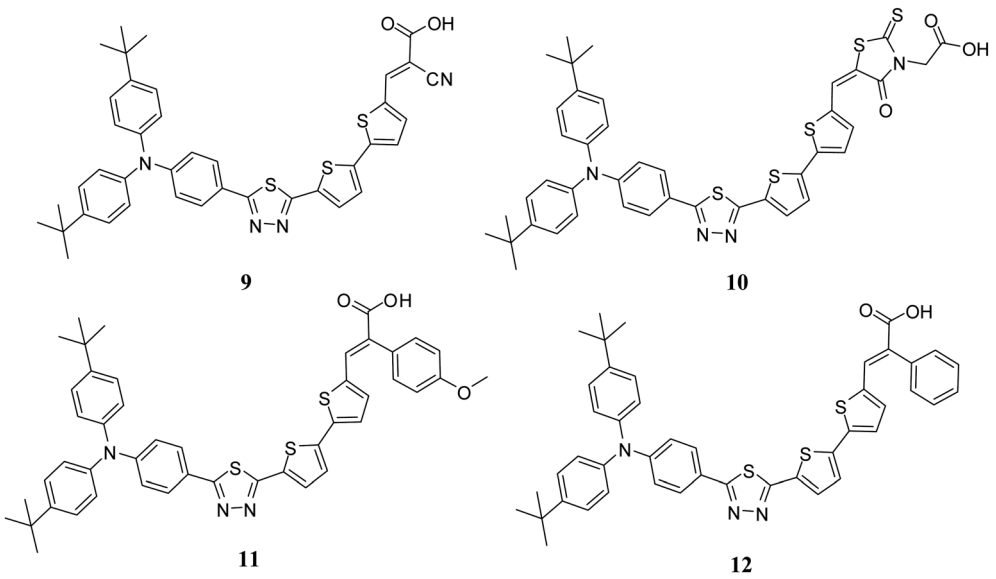

Scheme 1 Molecular structures of dyes **9–12**.

our knowledge this is the first report on thiadiazole containing DSSCs.

Results and discussion

Synthesis

All the dyes (**9–12**) were synthesized in multi-step synthetic pathway as shown in Scheme 2. 4-Aminobenzoic acid was esterified and then *N*-arylation conducted using bromo-4-*tert*-butylbenzene under modified Ullman conditions to get triarylamine derivative **3**. Hydrazine hydrate was reacted with triarylamine ester **3** to make *N*′-4-(bis(4-*tert*-butylphenyl)amino)benzohydrazide (**4**). Compound **4** further converted, by reacting with thiophene-2-carbonyl chloride to *N*′-(4-(bis(4-*tert*-butylphenyl)-amino)benzoyl)thiophene-2-carbohydrazide (**5**). The compound **5** was treated with Lawesson's reagent to produce thiadiazole derivative **6**, later it was converted into tributyl stannane derivative **7**. The tributyl stannane derivative **7** was coupled with 5-bromothiophene-2-carbaldehyde using standard Stille protocol to afford 5′-(5-(4-(bis(4-*tert*-butylphenyl)amino)phenyl)-1,3,4-thiadiazol-2-yl)-2,2′-bithiophene-5-carbaldehyde (**8**). The bithiophene-5-carbaldehyde derivative **8** was subjected to Knoevenagel condensation to produce the target dyes **9–12** in good yields.

Absorption and emission characteristics

The UV-Vis absorption spectra of the dyes **9–12** (1×10^{-5} M) were recorded in $CHCl_3$ (Fig. 1a) and the results are summarized in Table 1. All the four dyes display their absorption maxima in the visible region (400–490 nm). The observed visible region absorption is attributed to the intramolecular charge transfer between donor (triphenylamine) and acceptor (acid) groups. The dyes **11** and **12** show nearly equal absorption maxima, 444 nm and 443 nm respectively, whereas, the dyes **9** and **10** show red shifted absorption maxima 453 nm and 487 nm compared to **11** and **12**. The observed higher molar extinction coefficients of the dyes could result in the improved light harvesting capacity. Fluorescence emission spectra of the dyes **9–12** (1×10^{-5} M) were recorded in $CHCl_3$ solution (Fig. S1†) and the results are summarized in Table 1. All these dyes exhibit maximum emission wavelength in the range of 537–564 nm. The absorption and emission characteristics of the synthesized dyes were also measured in 1×10^{-5} M acetonitrile–*tert*-butyl alcohol (1 : 1) solvent mixture (Fig. S3†) and the results are summarized in Table S3.† In compare to spectra recorded in chloroform, all the molecules showed about 10 nm blue shift of absorption maxima (443–487 nm); **9**, **10**, and **11** showed red shift of 61, 12, and 20 nm respectively in maximum emission wavelength.

The absorption spectra of the dyes adsorbed on TiO_2 are shown in Fig. 1b. The absorption bands of dyes are broadened after their adsorption on TiO_2 surface compared to their solution spectra. This broad range of absorption can improve the light harvesting ability, photo current response region and short circuit current density (J_{sc}) of the solar cells. The absorption spectrum of the dyes are either blue or red shifted[42,43] compared to solution phase. The maximum red shift (40 nm) observed with **9**, may be attributed to J-aggregation of the dye on TiO_2 surface.[43] The dyes **10** and **12** displayed only a minimal shifts (1 and 4 nm in their absorption maxima) upon binding to TiO_2 and this indicates that the bulky phenyl group hindered their aggregation. The observed blue shift (8 nm) in the case of **11** might be attributed to the H-aggregation of dye on TiO_2 surface.[44]

Electrochemical properties

Electrochemical properties of the synthesized dyes were investigated using cyclic voltammetry (Fig. 2). All the dyes displayed nearly equal oxidation potentials (E_{OX}) ranging from 0.93–0.96 V and reduction potentials (E_{red}) ranging from −0.85 to −0.98 V (Table 1). The oxidation of TPA moiety is responsible for the observed oxidation potentials. Excited state oxidation potentials of

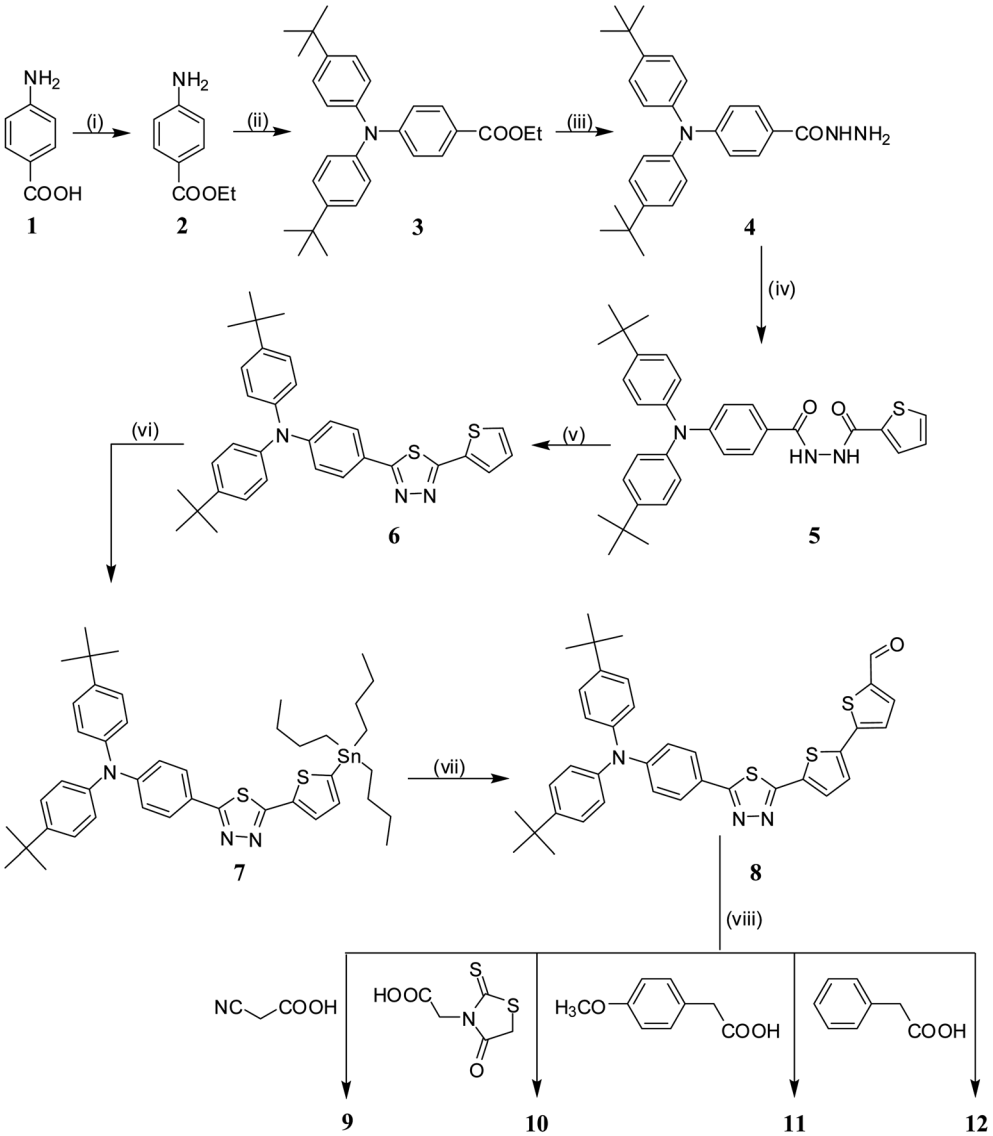

Scheme 2 Outline of synthetic scheme for **9–12**: (i) $SOCl_2$, EtOH, reflux, 6 h (ii) 1-bromo-4-*tert*-butylbenzene, 10 mol% 1,10-phenthroline, 20 mol% CuI, 2.5 eq. K_2CO_3, DMF, reflux, 48 h (iii) $NH_2NH_2{\cdot}H_2O$, EtOH, reflux, 17 h (iv) thiophene-2-carbonyl chloride, Et_3N, dry THF, RT, 16 h (v) Lawesson's reagent, dry THF, reflux, 5 h (vi) *n*-BuLi, Bu_3SnCl, dry THF, 6 h (vii) 5-bromothiophene-2-carbaldehyde, $Pd(PPh_3)_2Cl_2$, toluene, reflux, 14 h (viii) NH_4OAc, AcOH, reflux, 6 h.

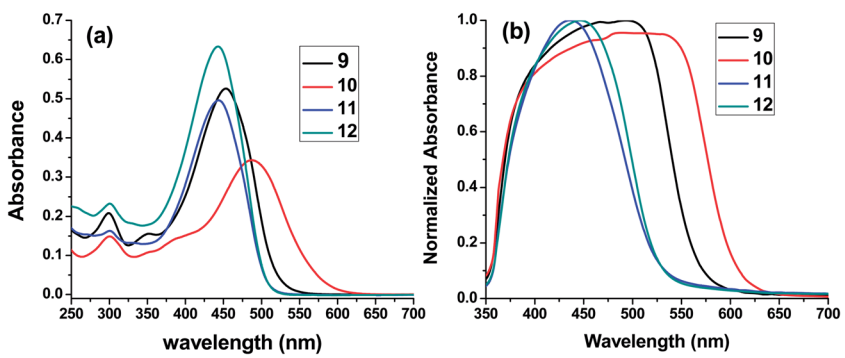

Fig. 1 The UV-visible spectra of the dyes in (a) solution (1×10^{-5} M in chloroform) and (b) thin film (adsorbed on TiO_2) state.

Table 1 Photophysical and electrochemical properties of the synthesized dyes **9–12**

Dye	λ_{max}[a]/nm (M^{-1} cm^{-1})	λ_{max}[b]/nm	λ_{max}[c]/nm	E_{OX}[d]/V (*vs.* SCE)	E_{red}[d]/V (*vs.* SCE)	E_{0-0}[e]/eV	E^*_{OX}[f]/V (*vs.* SCE)	Dye-loading amount (10^{-7} mol cm^{-2})
9	453 (54 679)	493	537	0.95	−0.85	2.47	−1.52	1.93
10	487 (34 299)	488	564	0.96	−0.95	2.38	−1.42	1.66
11	444 (49 617)	436	544	0.94	−0.96	2.45	−1.51	1.74
12	443 (63 304)	447	545	0.93	−0.98	2.45	−1.52	1.68

[a] Absorption maxima in $CHCl_3$ solution. [b] Absorption maxima on TiO_2 film. [c] Fluorescence emission maxima in $CHCl_3$. [d] Measured in CH_2Cl_2 with 0.1 M tetrabutylammonium hexafluorophosphate ($TBAPF_6$) as the electrolyte (working electrode: glassy carbon; reference electrode: SCE; calibrated with ferrocene/ferrocenium (Fc/Fc^+) as an external reference. Counter electrode: Pt wire). [e] E_{0-0} was estimated from the intersection between the absorption and emission spectra. [f] E^*_{OX} estimated by $E^*_{OX} = E_{OX} - E_{0-0}$.

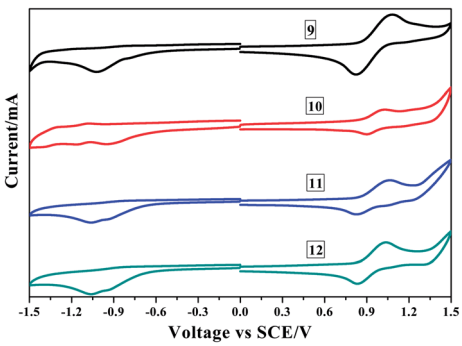

Fig. 2 Cyclic voltammograms of the dyes (5×10^{-4} M) in CH_2Cl_2.

the dyes (E^*_{OX}), which correspond to LUMO, are obtained by subtracting their oxidation potentials from optical band gap, which was derived from the intersection point of excitation and emission spectra. The ground state oxidation potentials (E_{OX}) of the dyes are more positive than I^-/I_3^- (0.2 V *vs.* SCE),[45] the electrolyte used in DSSCs, whereas, the calculated excited state oxidation potentials of the dyes (E^*_{OX}) (−1.42 to −1.52) are more negative compared to TiO_2 conduction band (−0.8 V *vs.* SCE).[46] These results confirm the feasibility of dye regeneration and electron injection processes.

Computational studies

The molecular orbital analysis was carried out for all four dyes in the gas phase at B3LYP/6-311G(d,p) level of theory. The electron density distribution for the HOMO, HOMO−1 and LUMO of **9–12** dyes are shown in Fig. 3. HOMO of all the four dyes is localized on the donor (TPA) moiety, whereas the LUMO it is localized on the A–π–A moiety. LUMO of **9**, **11** and **12** is localized on the carboxylic acid anchoring group, whereas in case of **10**, it has a larger contribution of the sulfur atom of rhodanine ring. The observed electron density distribution of the dyes on the bridging units in both HOMO and LUMO levels suggest effective photo-driven charge transfer excitation. The well separated electron density distribution of HOMO and LUMO levels indicated that the transition between these levels could be considered as a charge transfer excitation. TDDFT is used to study the excited states and the results show that the dyes have their absorption in the visible region. Of the functionals used M06-2X and CAM-B3LYP results are in good agreement with experimental data. The first two low energy transitions with high oscillator strengths and ground state dipole moments are listed in Table S1 and S2.† The low energy transition corresponds to an excitation from HOMO to LUMO as the major component and HOMO−1 to LUMO as a minor component. This mixing of HOMO−1 into the lowest energy transition decreases the charge transfer tendency.

Adsorption of dye on TiO_2 surface

To investigate the DSSC properties of the synthesized dyes, $Ti_{16}O_{32}$ nanocluster model is considered for TiO_2 as electron acceptor.[47,48]

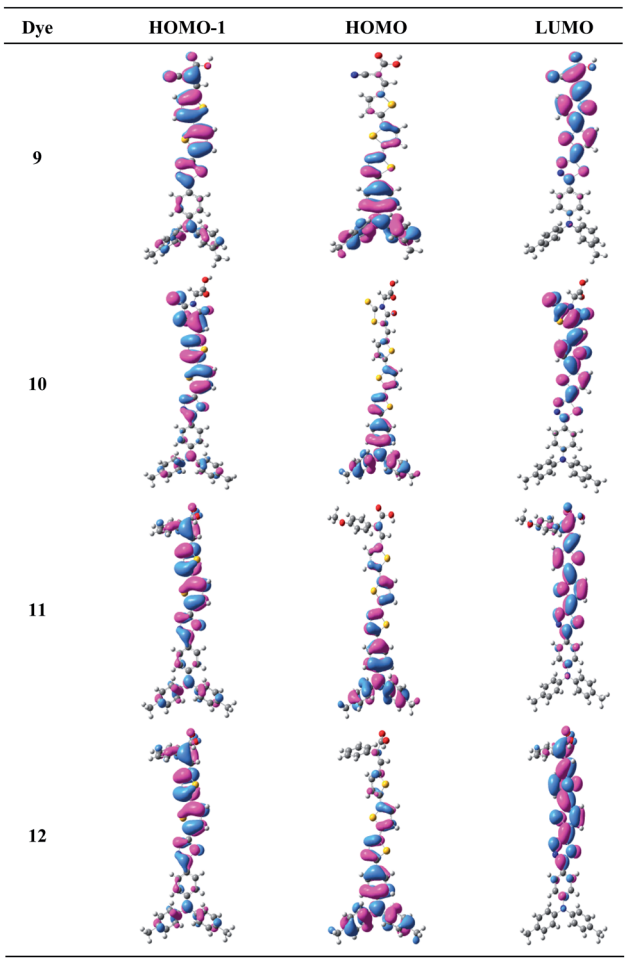

Fig. 3 Frontier molecular orbitals of dyes **9–10** obtained at B3LYP/6-31G(d,p) level.

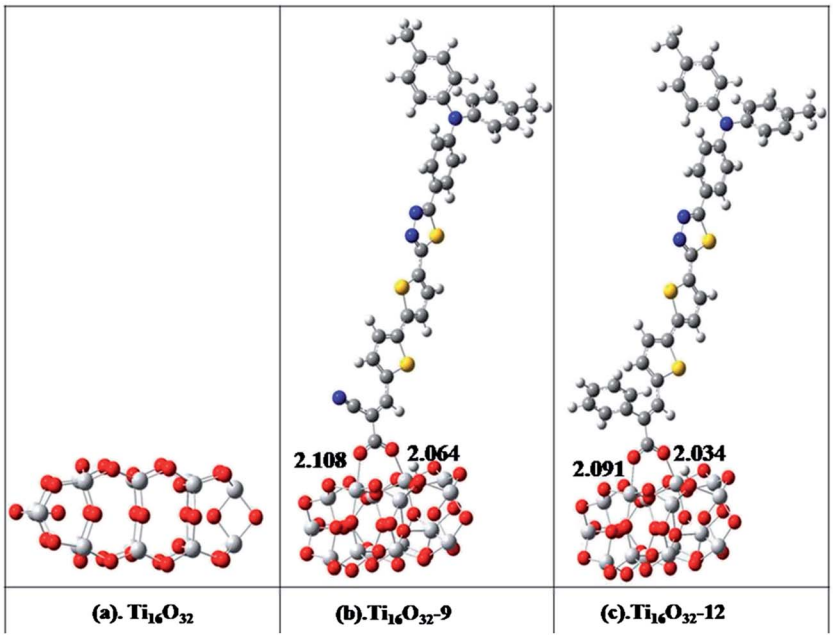

Fig. 4 Optimized bidentate bridging mode of the (a) $Ti_{16}O_{32}$, (b) $Ti_{16}O_{32}$-**9** (b), and (c) $Ti_{16}O_{32}$-**12**.

For the present work we considered the dye adsorbed on TiO_2 model in which the dye is attached to TiO_2 *via* bidentate bridging mode and the proton of the deprotonated acid group of the dye is attached to adjacent oxygen atom on TiO_2 surface as shown in Fig. 4. The dye molecule can anchor on to TiO_2 nanocluster surface through the acid group in various modes of adsorption, such as mono dentate, bidentate chelating and bidentate bridging mode. We considered only the bidentate bridging mode in this study as it is the strongest adsorption mode reported in the literature.[40,41,49,50] To validate the TiO_2 nanocluster model we calculated the adsorption energies for the molecules 9 and 12 using the formula ($E_{ads} = E_{molecule} + E_{TiO_2} - E_{molecule+TiO_2}$).[40,41] These are found to be 14.1 kcal mol^{-1} and 20.0 kcal mol^{-1} which are in the same range of the adsorption energies of molecules with similar anchoring groups using larger TiO_2 clusters.[51]

To understand the electron density in the molecules, density of states (DOS) is calculated for $Ti_{16}O_{32}$ alone and the dye adsorbed $Ti_{16}O_{32}$ and the results are depicted in Fig. S2.† The results show that DOS of $Ti_{16}O_{32}$ alone has very broad surface and the valence and conduction bands are separated by wide band gap. Whereas in dye adsorbed $Ti_{16}O_{32}$, the valence and conduction band gap is decreased due to the introduction of dye occupied molecular energy levels. The DOS analysis reveals that all the dyes exhibited a strong overlap of the valence and conduction bands over a broad range of energies. From frontier molecular orbital analysis of the dye adsorbed on to TiO_2 surface (Fig. 5) it is clear that on excitation electron density is transferred from HOMO of dye to its LUMO and from there to LUMO of the semiconductor, indicating the efficient interfacial electron injection from excited dye to semiconductor.

Photovoltaic performance of DSSCs

The IPCE action spectrum of the dye is shown in Fig. 6 and the results indicate that all the dyes can efficiently convert the light to photocurrent in the region from 300 to 650 nm. The onsets of the IPCE spectra (640, 660, 580 and 585 nm, respectively for 9, 10, 11 and 12) are significantly broadened compared to their UV-Vis absorption spectra on the TiO_2 film. The photocurrents measured at wavelengths less than 400 nm may have contributions from the direct excitation of TiO_2 and competitive light absorption triiodide (I_3^-) in the electrolyte solution; however, those at longer wavelengths are reasonably attributed to sensitization by the indicated sensitizer. The DSSC in which 9 is used as dye, showed more than 60% IPCE in the range 350–550 nm and it is the highest among the four. This might be due to the

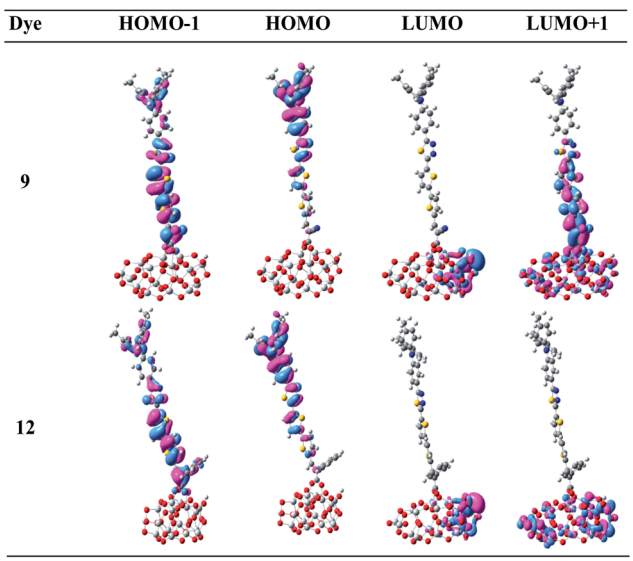

Fig. 5 Frontier molecular orbitals of dyes **9** and **12** adsorbed on $Ti_{16}O_{32}$ obtained at PBE0/TZVP level.

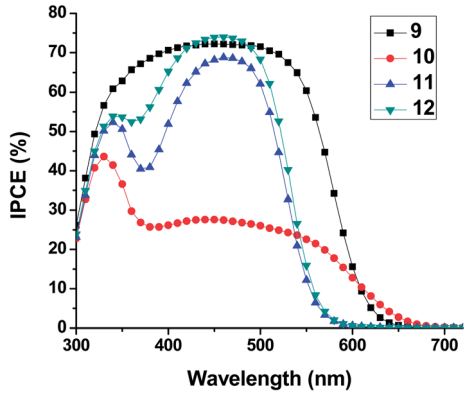

Fig. 6 IPCE action spectra of DSSCs based on **9–12** dyes.

wide range of absorption of 9 adsorbed on TiO_2 film. The IPCE values of the DSSCs based on 11 and 12 dyes displayed more than 60% in the range of 420–510 nm and 380–520 nm, respectively. The strong dip in the IPCE spectrum around 380 nm for compound **11** is induced by the competitive light absorption between sensitizer and triiodide. Interestingly, the DSSC with 10 dye portrayed low IPCE value, even though it has a broader range of absorption. The reason behind the observed low IPCE value at wavelengths higher than 400 nm for compound **10** is explained using computational experiments. The energetically stable conformer of 10 showed that its LUMO was located on rhodanine sulfur atom instead of carboxylic acid moiety, which reduced the electron transfer from the dye to the TiO_2 conduction band and hence minimized the IPCE. The high photocurrents measured in the range of 300–380 nm may have contributions from the direct excitation of TiO_2 and hot electron injection from higher excited state of the sensitizer.

The photocurrent density–photovoltage (*J–V*) curves of the DSSCs with **9–12** dyes, under simulated AM 1.5 solar irradiation (100 mW cm^{-2}) is shown in Fig. 7 and their photovoltaic properties are summarized in Table 2.

Among all, the DSSC with dye **9** showed highest efficiency ($\eta = 4.12\%$), with short-circuit current density (J_{sc}) of 8.50 mA cm^{-2}, open-circuit voltage (V_{oc}) of 645 mV and fill factor (FF) of

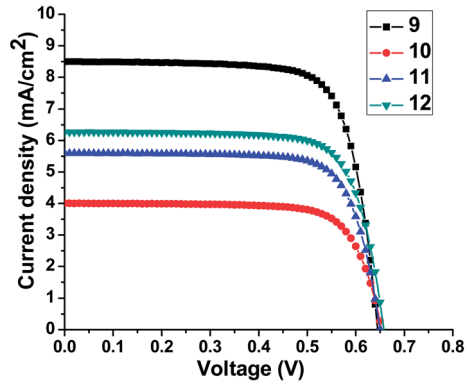

Fig. 7 *J–V* characteristics of DSSCs fabricated using **9–12** as dyes under AM 1.5 solar irradiation.

Table 2 Photovoltaic performance of DSSCs fabricated using **9–12**

Dye	J_{sc} (mA cm^{-2})	V_{oc} [V]	FF	PCE (%)
9	8.50	0.645	0.75	4.12
10	4.0	0.654	0.74	1.95
11	5.59	0.650	0.75	2.74
12	6.27	0.658	0.75	3.10

0.75. Whereas, the DSSC with **10** dye displayed the lowest efficiency $\eta = 1.95\%$ due to its low short-circuit current density ($J_{sc} = 4.00$ mA cm^{-2}). The observed low J_{sc} might be due to the poor electron injection nature of **10** to the TiO_2 conduction band. The DSSCs with **11** and **12** dyes exhibited comparable efficiencies ($\eta = 2.74$ and 3.10%, respectively for **11** and **12**).

Experimental

Materials and instruments

All the materials for synthesis were purchased from commercial suppliers and used without further purification. Dry DMF (dried over molecular sieves) and freshly distilled THF (distilled over sodium/benzophenone) were used in all experiments. NMR spectra were recorded using Bruker Avance (300 MHz) or Varian Inova (500 MHz) spectrometers. ESI MS spectra were obtained on a Thermofinngan Mass Spectrometer. Absorption spectra were recorded on a Jasco V-550 UV-visible spectrophotometer. Fluorescence measurements were performed on a Fluorolog-3 fluorescence spectrophotometer. Cyclic voltammetric measurements were performed on a PC-controlled CHI 620C electrochemical analyzer using 0.5 mM dye solution in dichloromethane (CH_2Cl_2) at a scan rate of 100 mV s^{-1}. Tetrabutylammonium hexafluorophosphate (0.1 M) was used as supporting electrolyte. The glassy carbon, standard calomel electrode (SCE) and platinum wire were used as working, reference and counter electrodes, respectively. The potential of reference electrode was calibrated using ferrocene internal standard. All the potentials were reported against SCE. All measurements were carried out at room temperature.

DSSC characterization

Screen printing method was used to prepare a nanocrystalline TiO_2 (thickness 25 nm, area: 0.25 cm^2) as described earlier.[52] The dye solution (3×10^{-4} M) was prepared in acetonitrile–*tert*-butyl alcohol (1 : 1 v/v) and to prevent aggregation of the dye molecules, deoxycholic acid (DCA) (20 mM) was used as a co-adsorbent. The TiO_2 films were dipped into the dye solution and kept at 25 °C for 24 h. Acetonitrile solution, contained 0.6 M dimethylpropyl-imidazolium iodide (DMPII), I_2 (0.05 M), LiI (0.1 M) and 0.5 M *tert*-butylpyridine (TBP) was used as electrolyte. A Surlyn spacer with 40 μm thickness was used to separate the counter electrode and dye-deposited TiO_2 film, sealed with polymer frame. The photocurrent density–voltage (*I–V*) characteristics of the sealed solar cells were measured under AM 1.5 G simulated solar light with light intensity of 100 mW cm^{-2} and a

metal mask of 0.25 cm^2. These *I–V* characteristics were used to estimate the photovoltaic parameters.

Measurement of dye-loading

The adsorption amount of dyes on the surface of TiO_2 films, that were prepared under the same conditions as those fabricated into cells, was estimated as follows: TiO_2 films sensitized with dyes were immersed into 0.1 M NaOH in THF–H_2O (1/1, v/v) for desorption of the dyes. The amount of adsorbed dye was estimated from the absorption peak of each resulting solution. Four pieces of TiO_2 film for one cell were tested and an average value was adopted.

Computational studies

Ground state geometry of all the four dyes (**9** to **12**) were optimized using density functional theory B3LYP/6-311G(d,p) method. Vibrational analysis was carried out to check the geometries optimized to be local minima. TD-DFT calculations were performed on the optimized geometries for the first singlet excited states to estimate the first excitation energy for the dyes using various functionals like M06-2X, CAM-B3LYP, LC-BLYP, LC-WPBE, and WB97XD with 6-311+G(d,p) basis set in solvent chloroform phase using SCRF(PCM) method.[53] The ground state geometry of $Ti_{16}O_{32}$ nanocluster alone and dye absorbed $Ti_{16}O_{32}$ nanocluster was optimized using PBE0 functional[54] and TZVP[55] basis set. Density of states was analyzed using GaussSum2.2 program.[56] All the calculations were performed using G09 software.[57]

Synthesis

Ethyl 4-(bis(4-*tert*-butylphenyl)amino)benzoate (3). To the mixture of 1-bromo-4-*tert*-butylbenzene (17.0 g, 80 mmol) and ethyl 4-aminobenzoate[58] (6.0 g, 36 mmol) in 50 mL of DMF, crushed K_2CO_3 (12.5 g, 90.7 mmol) and CuI (1.38 g, 7.2 mmol) were added, sonicated under nitrogen atmosphere. After for 20 minutes, 1,10-phenathroline (0.67 g, 3.6 mmol) was added to the reaction mixture and it was refluxed under nitrogen atmosphere for 48 h. After completion of the reaction monitored using TLC, the reaction mixture was cooled, concentrated under reduced pressure. Ethyl acetate (100 mL) was added and the solution was filtered through a small pad of silica gel. The filtrate was concentrated and purified by column chromatography (silica gel 60–120 mesh and 2 : 98 ethyl acetate–petroleum ether as eluent) to afford desired product as white solid (isolated yield: 60%, 9.3 g): ^{1}H NMR ($CDCl_3$, 300 MHz): δ 7.79 (d, J = 9.06 Hz, 2H), 7.26 (d, J = 8.30 Hz, 4H), 7.02 (d, J = 8.30 Hz, 4H), 6.92 (d, J = 9.06 Hz, 2H), 4.31 (q, J = 6.79 Hz, 2H), 1.36 (t, J = 6.79 Hz, 3H), 1.32 (s, 18H). ^{13}C NMR ($CDCl_3$, 75 MHz): δ 166.41, 152.17, 147.24, 143.84, 130.65, 126.27, 125.61, 121.61, 119.06, 60.29, 34.35, 31.36, 14.39. ESI-MS: m/z 430 ($[M + H]^+$). HRMS (ESI+) calcd for $C_{29}H_{36}O_2N$ $[M + H]^+$ 430.2740 found 430.2738.

4-(Bis(4-*tert*-butylphenyl)amino)benzohydrazide (4). To the solution of hydrazine monohydrate (3.0 g, 60 mmol) in ethanol (50 mL), **3** (5.0 g, 11.6 mmol) was added portion wise and the mixture was refluxed for 17 h. After completion of the reaction as monitored using TLC, ethanol was removed under reduced pressure and added water to the residue resulted in the formation of white solid. The solid was filtered and re-crystallized from ethanol to afford pure product as white solid (isolated yield: 3.8 g, 80%). ^{1}H NMR ($CDCl_3$, 300 MHz): δ 7.55 (d, J = 8.68 Hz, 2H), 7.24 (d, J = 8.68 Hz, 4H), 7.0 (d, J = 8.68 Hz, 4H), 6.94 (d, J = 8.68 Hz, 2H), 4.79 (brs, NH_2, 2H), 1.31 (s, 18H). ^{13}C NMR ($CDCl_3$, 75 MHz): δ 168.42, 151.41, 147.09, 143.83, 127.88, 126.27, 125.16, 123.51, 119.63, 34.33, 31.34. ESI-MS: m/z 416 ($[M + H]^+$). HRMS (ESI+) calcd for $C_{27}H_{34}ON_3$ $[M + H]^+$ 416.2696 found 416.2693.

***N*′-(4-(Bis(4-*tert*-butylphenyl)amino)benzoyl)thiophene-2-carbohydrazide (5).** To the mixture of **4** (7.0 g, 16.8 mmol) and triethylamine (5.09 g, 50.4 mmol) in dry THF at 0 °C, thienyl chloride (2.4 g, 16.8 mmol) was added drop wise. After the addition, the reaction mixture was allowed to stir at room temperature for 16 h. After the complete consumption of **4**, water (20 mL) followed by a saturated solution of sodium bicarbonate (20 mL) was added to the reaction mixture. The water phase was extracted with ethyl acetate (3 × 25 mL) and the combined organic fractions were washed with brine (25 mL), dried over anhydrous sodium sulfate. The solvent was removed *in vacuo* and re-crystallized from ethanol to yield the desired product as a white solid (isolated yield: 7.7 g, 87%). ^{1}H NMR ($CDCl_3$ + DMSO-d_6, 300 MHz): δ 10.33 (s, 1H), 10.15 (s, 1H), 7.89 (d, J = 3.77 Hz, 1H), 7.78 (d, J = 8.68 Hz, 2H), 7.60 (d, J = 5.09 Hz, 1H), 7.29 (d, J = 8.68 Hz, 4H), 7.12 (dd, J = 5.09 Hz, 3.77), 7.03 (d, J = 8.68 Hz, 4H), 6.95 (d, J = 8.68 Hz, 2H), 1.32 (s, 18H). ^{13}C NMR ($CDCl_3$, 75 MHz): δ 170.69, 166.39, 156.23, 152.23, 149.14, 138.84, 134.24, 133.48, 131.95, 130.66, 124.31, 39.67, 36.72. ESI-MS: m/z 526 ($[M]^+$). HRMS (ESI+) calcd for $C_{32}H_{35}N_3O_2S$ $[M + H]^+$ 525.2450 found 526.2520.

4-*tert*-Butyl-*N*-(4-*tert*-butylphenyl)-*N*-(4-(5-(thiophen-2-yl)-1,3,4-thiadiazol-2-yl)phenyl)aniline (6). Lawesson's reagent (2.3 g, 5.7 mmol) was added to **5** (3.0 g, 5.7 mmol) in dry THF (30 mL) and the mixture was stirred under reflux at 80 °C for 5 h. After completion of the reaction as monitored by TLC, the crude product was chromatographed on silica gel (60–120 mesh) using ethyl acetate–hexane (3 : 97; v/v) as eluent to afford the product in pure form as yellow solid (isolated yield: 2.3 g, 80%). ^{1}H NMR ($CDCl_3$, 500 MHz): δ 7.77 (d, J = 9.16 Hz, 2H), 7.54 (d, J = 3.66 Hz, 1H), 7.45 (d, J = 5.49 Hz, 1H), 7.30 (d, J = 8.24 Hz, 4H), 7.11 (dd, J = 3.66 Hz, 5.49, 1H), 7.07 (d, J = 8.24 Hz, 4H), 7.05 (d, J = 9.16 Hz, 2H), 1.35 (s, 18H). ^{13}C NMR ($CDCl_3$, 75 MHz): δ 167.39, 160.47, 150.81, 147.16, 143.83, 132.74, 129.10, 128.85, 128.72, 127.84, 126.31, 125.16, 121.54, 120.39, 34.36, 31.37. ESI-MS: m/z 524 ($[M]^+$). HRMS (ESI+) calcd for $C_{32}H_{34}N_3S_2$ $[M + H]^+$ 524.2188 found 524.2190.

5′-(5-(4-(Bis(4-*tert*-butylphenyl)amino)phenyl)-1,3,4-thiadiazol-2-yl)-2,2′-bithiophene-5-carbaldehyde (8). Under argon atmosphere, *n*-butyllithium (1.6 M, 1.24 mL, 2.0 mmol) was added drop wise to **6** (1.0 g, 1.9 mmol) in 15 mL of anhydrous THF at −78 °C. After stirring for 1 h at −78 °C, tributylstannyl chloride (0.78 g, 2.4 mmol) was added and temperature was raised to room temperature, stirred for 6 h. After complete consumption of the starting material, the reaction was terminated with water. The mixture was extracted with

dichloromethane, dried over anhydrous sodium sulfate, filtered and concentrated under reduced pressure to obtain **7** as brown oil and it was used as it is for further reaction. To the mixture of **7** (1.0 g, 1.2 mmol) and $Pd(PPh_3)_2Cl_2$ (0.13 g, 0.19 mmol) in toluene (20 mL), 5-bromothiophene-2-carbaldehyde (0.38 g, 2.0 mmol) was added and the mixture was refluxed for 14 h at 110 °C under argon atmosphere. After completion of the reaction, the mixture was partitioned between ethyl acetate and water, ethyl acetate layer was collected, washed with brine and dried over anhydrous sodium sulfate. After removing solvent under reduced pressure, the residue was purified by column chromatography (silica gel 60–120 mesh and 1 : 10 ethyl acetate–petroleum ether as eluent) on to yield the product as red solid (isolated yield: 0.68 g, 90%). ^{1}H NMR ($CDCl_3$, 500 MHz): δ 9.87 (s, 1H), 7.75 (d, J = 8.65 Hz, 2H), 7.66 (d, J = 3.84 Hz, 1H), 7.44 (d, J = 4.81 Hz, 1H), 7.33 (dd, J = 3.84 Hz, 4.81, 1H), 7.28 (d, J = 8.65 Hz, 4H), 7.25 (s, 2H), 7.07 (s, 2H), 7.06 (d, J = 8.65 Hz, 4H), 7.02 (s, 1H) 1.33 (s, 18H). ^{13}C NMR ($CDCl_3$, 75 MHz): δ 182.65, 167.95, 159.87, 151.01, 147.31, 145.65, 144.80, 143.75, 142.50, 139.43, 138.77, 137.33, 133.76, 132.20, 129.93, 128.82, 126.48, 125.29, 121.30, 120.17, 34.40, 31.37. ESI-MS: m/z 634 ($[M]^+$). HRMS (ESI+) calcd for $C_{37}H_{39}O_2N_3S_3$ $[M + H]^+$ 634.20044 found 634.2033.

General procedure for synthesis of 9–12

To the solution of carbaldehyde **8** (1 g, 1.5 mmol) and ammonium acetate (5.7 mg, 0.07 mmol) in acetic acid (20 mL), 4.5 mmol of 2-cyanoacetic acid (0.38 g), rhodanine-3-acetic acid (0.86 g, 4.5 mmol), 2-(4-methoxyphenyl)acetic acid (0.74 g, 4.5 mmol) or 2-phenylacetic acid (0.61 g, 4.5 mmol) was added. The resultant mixture was refluxed for 4 h and the progress of the reaction was monitored using TLC. After completion, the reaction mixture was cooled and the precipitate formed was filtered, washed sequentially with water, cold methanol and with hexane–diethylether (1 : 1) mixture. Further, the precipitate was re-crystallized from toluene-methanol mixture to afford the target compounds **9–11** or **12** in pure form.

3-(5′-(5-(4-(Bis(4-*tert*-butylphenyl)amino)phenyl)-1,3,4-thiadiazol-2-yl)-2,2′-bithiophen-5-yl)-2-cyanoacrylic acid (9). Red solid (isolated yield: 0.63 g, 60%). ^{1}H NMR (DMSO-d_6, 300 MHz): δ 8.42 (s, 1H), 8.11 (s, 1H), 7.91 (d, J = 4.15 Hz, 1H), 7.75 (d, J = 8.68 Hz, 2H), 7.67 (d, J = 3.96 Hz, 1H), 7.58 (m, 1H), 7.33 (d, J = 8.68 Hz, 4H), 7.06 (d, J = 8.68 Hz, 4H), 6.98 (d, J = 8.68 Hz, 2H), 1.32 (s, 18H). ^{13}C NMR ($CDCl_3$, 75 MHz): δ 167.41, 163.43, 159.08, 154.18, 150.49, 146.88, 145.50, 144.19, 143.14, 139.53, 138.01, 135.08, 132.82, 130.61, 129.17, 128.59, 127.95, 126.74, 125.54, 124.06, 121.05, 116.05, 33.99, 31.03. ESI-MS: m/z 699 ($[M - H]^-$). HRMS (ESI+) calcd for $C_{40}H_{37}O_2N_4S_3$ 701.2073 $[M + H]^+$ found 701.2092.

2-(5-((5′-(5-(4-(Bis(4-*tert*-butylphenyl)amino)phenyl)-1,3,4-thiadiazol-2-yl)-2,2′-bithiophen-5-yl)methylene)-4-oxo-2-thioxothiazolidin-3-yl)acetic (10). Red solid (isolated yield: 0.7 g, 58%). ^{1}H NMR (DMSO-d_6, 300 MHz): δ 8.17 (s, 1H), 7.85–7.80 (m, 4H), 7.74 (d, J = 3.96 Hz, 1H), 7.70 (d, J = 3.96 Hz, 1H), 7.42 (d, J = 8.49 Hz, 4H), 7.09 (d, J = 8.49 Hz, 4H), 6.91 (d, J = 8.87 Hz, 2H), 4.72 (s, 2H), 1.29 (s, 18H). ESI-MS: m/z 805 ($[M - H]^-$). HRMS (ESI+) calcd for $C_{44}H_{39}O_3N_4S_5$ $[M + H]^+$ 807.1627 found 807.1639.

3-(5′-(5-(4-(Bis(4-*tert*-butylphenyl)amino)phenyl)-1,3,4-thiadiazol-2-yl)-2,2′-bithiophen-5-yl)-2-(4-methoxyphenyl)acrylic acid (11). Orange-red solid (isolated yield: 065 g, 56%) ^{1}H NMR ($CDCl_3$, 300 MHz): δ 8.04 (s, 1H), 7.77–7.73 (m, 2H), 7.36 (d, J = 4.53 Hz, 1H), 7.34–7.30 (m, 4H), 7.22 (d, J = 8.30 Hz, 2H), 7.20–7.16 (m, 2H), 7.13 (d, J = 4.53 Hz, 1H), 7.08 (d, J = 8.30 Hz, 4H), 7.05–7.01 (m, 4H), 3.90 (s, 3H) 1.32 (s, 18H). ^{13}C NMR ($CDCl_3$, 75 MHz): δ 172.30, 167.54, 160.13, 159.91, 150.89, 147.24, 143.76, 141.37, 139.81, 138.49, 135.25, 132.01, 131.17, 129.80, 128.77, 128.28, 126.15, 125.21, 125.01, 124.29, 121.28, 120.25, 114.76, 113.88, 55.33, 34.39, 31.37. ESI-MS: m/z 780 ($[M - H]^-$). HRMS (ESI+) calcd for $C_{46}H_{43}O_3N_3S_3$ $[M + H]^+$ 782.2515 found 782.2545.

3-(5′-(5-(4-(Bis(4-*tert*-butylphenyl)amino)phenyl)-1,3,4-thiadiazol-2-yl)-2,2′-bithiophen-5-yl)-2-phenylacrylic acid (12). Orange-red solid (isolated yield: 0.63 g, 56%). ^{1}H NMR ($CDCl_3$, 300 MHz): δ 8.06 (s, 1H), 7.74 (d, J = 8.30, *2*H), 7.52–7.49 (m, 3H), 7.36–7.28 (m, 7H), 7.17–7.12 (m, 2H), 7.10–7.02 (m, 5H), 7.02–6.98 (m, 2H) 1.32 (s, 18H). ^{13}C NMR ($CDCl_3$, 75 MHz): δ 171.72, 160.05, 159.89, 150.90, 147.25, 143.76, 141.58, 139.75, 138.26, 135.36, 135.28, 134.23, 132.07, 129.81, 129.38, 129.08, 128.77, 128.59, 128.46, 127.70, 126.36, 125.21, 124.92, 124.23, 121.28, 120.26, 34.40, 31.37. ESI-MS: m/z 751 ($[M - H]^-$). HRMS (ESI+) calcd for $C_{46}H_{43}O_2N_3S_3$ $[M + H]^+$ 752.2469 found 752.2439.

Conclusions

Four new D–A–π–A type organic dyes with different acceptor/anchor groups were synthesized, characterized, their photophysical, electrochemical and photovoltaic properties were explored. All the dyes showed their absorption in the visible region and exhibited good light harvesting capacity. The oxidation potentials of the dyes are more positive than I^-/I_3^- (0.2 V *vs.* SCE) and the calculated excited state oxidation potentials are more negative compared to TiO_2 conduction band (−0.8 V *vs.* SCE). The importance of the localization of the LUMO electron density on the acid/anchor group for better interfacial electron injection from excited state dye to semiconductor is also explored by DFT and TDDFT calculations and all the dyes exhibited efficient interfacial electron transfer. Under AM 1.5 irradiation, all the dyes showed moderate to good efficiencies. Among all, the DSSC with **9** dye showed highest efficiency (η = 4.12%), with short-circuit current density (J_{sc}) of 8.504 mA cm^{-2}, open-circuit voltage (V_{oc}) of 645 mV and fill factor (FF) of 0.75. The structural modification of **9** is in progress for further improvement in its photophysical and photovoltaic properties.

Acknowledgements

We thank the Director CSIR-IICT for the encouragement. We acknowledge funding from NWP-0054 project. GSK, KS, BS and DB thank CSIR for fellowships.

References

1 B. O'Regan and M. Gratzel, *Nature*, 1991, **353**, 737.
2 Y. Numata, S. P. Singh, A. Islam, M. Iwamura, A. Imai, K. Nozaki and L. Han, *Adv. Funct. Mater.*, 2013, **23**, 1817.
3 W. Zeng, Y. Cao, Y. Bai, Y. Wang, Y. Shi, M. Zhang, F. Wang, C. Pan and P. Wang, *Chem. Mater.*, 2010, **22**, 1915.
4 Y. S. Yen, H. H. Chou, Y. C. Chen, C. Y. Hsu and J. T. Lin, *J. Mater. Chem.*, 2012, **22**, 8734.
5 A. Mishra, M. K. R. Fischer and P. Bäuerle, *Angew. Chem., Int. Ed.*, 2009, **48**, 2474.
6 Y. Liang, B. Peng, J. Liang, Z. Tao and J. Chen, *Org. Lett.*, 2010, **12**, 1204.
7 J. H. Yum, D. P. Hagberg, S. J. Moon, K. M. Karlsson, T. Marinado, L. C. Sun, A. Hagfeldt, M. K. Nazeeruddin and M. Gratzel, *Angew. Chem., Int. Ed.*, 2009, **48**, 1576.
8 D. P. Hagberg, J. H. Yum, H. Lee, F. De Angelis, T. Marinado, K. M. Karlsson, R. Humphry-Baker, L. C. Sun, A. Hagfeldt, M. Gratzel and M. K. Nazeeruddin, *J. Am. Chem. Soc.*, 2008, **130**, 6259.
9 N. Koumura, Z. S. Wang, S. Mori, M. Miyashita, E. Suzuki and K. Hara, *J. Am. Chem. Soc.*, 2006, **128**, 14256.
10 D. Kuang, S. Uchida, R. H. Baker, S. M. Zakeeruddin and M. Grätzel, *Angew. Chem., Int. Ed.*, 2008, **47**, 1923.
11 Y. Wu, M. Marszalek, S. M. Zakeeruddin, Q. Zhang, H. Tian, M. Gratzel and W. Zhu, *Energy Environ. Sci.*, 2012, **5**, 8261.
12 K. Hara, M. Kurashige, Y. Dan-oh, C. Kasada, A. Shinpo, S. Suga, K. Sayama and H. Arakawa, *New J. Chem.*, 2003, **27**, 783.
13 K. Hara, K. Sayama, Y. Ohga, A. Shinpo, S. Suga and H. Arakawa, *Chem. Commun.*, 2001, 569.
14 P. J. Skabara, R. Berridge, I. M. Serebryakov, A. L. Kanibolotsky, L. Kanibolotskaya, S. Gordeyev, I. F. Perepichka, N. S. Sariciftci and C. Winder, *J. Mater. Chem.*, 2007, **17**, 1055.
15 H. Qin, S. Wenger, M. F. Xu, F. F. Gao, X. Y. Jing, P. Wang, S. M. Zakeeruddin and M. Gratzel, *J. Am. Chem. Soc.*, 2008, **130**, 9202.
16 J. Zhang, H. B. Li, S. L. Sun, Y. Geng, Y. Wu and Z. M. Su, *J. Mater. Chem.*, 2012, **22**, 568.
17 H. Tian, X. Yang, R. Chen, Y. Pan, L. Li, A. Hagfeldt and L. Sun, *Chem. Commun.*, 2007, 3741.
18 K. Hara, T. Sato, R. Katoh, A. Furube, T. Yoshihara, M. Murai, M. Kurashige, S. Ito, A. Shinpo, S. Suga and H. Arakawa, *Adv. Funct. Mater.*, 2005, **15**, 246.
19 D. P. Hagberg, T. Edvinsson, T. Marinado, G. Boschloo, A. Hagfeldt and L. C. Sun, *Chem. Commun.*, 2006, 2245.
20 S. Hwang, J. H. Lee, C. Park, H. Lee, C. Kim, C. Park, M. H. Lee, W. Lee, J. Park, K. Kim, N. G. Park and C. Kim, *Chem. Commun.*, 2007, 4887.
21 H. Choi, C. Baik, S. O. Kang, J. Ko, M. S. Kang, M. K. Nazeeruddin and M. Gratzel, *Angew. Chem., Int. Ed.*, 2008, **47**, 327.
22 K. R. J. Thomas, Y.-C. Hsu, J. T. Lin, K.-M. Lee, K.-C. Ho, C.-H. Lai, Y.-M. Cheng and P.-T. Chou, *Chem. Mater.*, 2008, **20**, 1830.
23 Q. Feng, X. Lu, G. Zhou and Z.-S. Wang, *Phys. Chem. Chem. Phys.*, 2012, **14**, 7993.
24 H. N. Tian, X. C. Yang, R. K. Chen, R. Zhang, A. Hagfeldt and L. Sun, *J. Phys. Chem. C*, 2008, **112**, 11023.
25 Y. Z. Wu and W. H. Zhu, *Chem. Soc. Rev.*, 2013, **42**, 2039.
26 W. H. Zhu, Y. Z. Wu, S. T. Wang, W. Q. Li, X. Li, J. Chen, Z. S. Wang and H. Tian, *Adv. Funct. Mater.*, 2011, **21**, 756.
27 S. Haid, M. Marszalek, A. Mishra, M. Wielopolski, J. Teuscher, J. Moser, R. Humphry-Baker, S. M. Zakeeruddin, M. Gratzel and P. Bauerle, *Adv. Funct. Mater.*, 2012, **22**, 1291.
28 J. Kim, H. Choi, J. Lee, M. Kang, K. Song, S. O. Kang and J. Ko, *J. Mater. Chem.*, 2008, **18**, 5223.
29 Y. Z. Wu, X. Zhang, W. Q. Li, Z. S. Wang, H. Tian and W. H. Zhu, *Adv. Energy Mater.*, 2012, **2**, 149.
30 Y. Cui, Y. Z. Wu, X. F. Lu, X. Zhang, G. Zhou, F. B. Miapeh, W. H. Zhu and Z. S. Wang, *Chem. Mater.*, 2011, **23**, 4394.
31 J. Y. Mao, F. L. Guo, W. J. Ying, W. J. Wu, J. Li and J. L. Hua, *Chem.–Asian J.*, 2012, **7**, 982.
32 K. Pei, Y. Z. Wu, W. J. Wu, Q. Zhang, B. Q. Chen, H. Tian and W. H. Zhu, *Chem.–Eur. J.*, 2012, **18**, 8190.
33 S. Y. Qu, W. J. Wu, J. L. Hua, C. Kong, Y. T. Long and H. Tian, *J. Phys. Chem. C*, 2010, **114**, 1343.
34 S. Y. Qu, C. J. Qin, A. Islam, Y. Z. Wu, W. H. Zhu, J. L. Hua, H. Tian and L. Y. Han, *Chem. Commun.*, 2012, **48**, 6972.
35 X. F. Lu, G. Zhou, H. Wang, Q. Y. Feng and Z. S. Wang, *Phys. Chem. Chem. Phys.*, 2012, **14**, 4802.
36 C. Chen, Y. Hsu, H. Chou, K. R. J. Thomas, J. T. Lin and C. Hsu, *Chem.–Eur. J.*, 2010, **16**, 3184.
37 J. X. He, W. J. Wu, J. L. Hua, Y. H. Jiang, S. Y. Qu, J. Li, Y. T. Long and H. Tian, *J. Mater. Chem.*, 2011, **21**, 6054.
38 Y. Z. Wu, M. Marszalek, S. M. Zakeeruddin, Q. Zhang, H. Tian, M. Gratzel and W. H. Zhu, *Energy Environ. Sci.*, 2012, **5**, 8261.
39 K. Srinivas, K. Yesudas, K. Bhanuprakash, V. Jayathirtha Rao and L. Giribabau, *J. Phys. Chem. C*, 2009, **113**, 20117.
40 K. Srinivas, Ch. R. Kumar, M. Ananth Reddy, K. Bhanuprakash, V. Jayathirtha Rao and L. Giribabu, *Synth. Met.*, 2010, **161**, 96.
41 K. Srinivas, G. Sivakumar, Ch. R. Kumar, M. Ananth Reddy, K. Bhanuprakash, V. Jayathirtha Rao, C. W. Chenc, Y. C. Hsuc and J. T. Lin, *Synth. Met.*, 2011, **161**, 1671.
42 S. G. Bairu, E. Mghanga, J. A. Hasan, S. Kola, K. Bhanuprakash, V. Jayathirtha Rao, L. Giribabu, G. P. Wiederrecht, R. da Silva, L. G. C. Rego and G. Ramakrishna, *J. Phys. Chem. C*, 2013, **117**, 4824.
43 M. Guo, P. Y Diao, J. Ren, F. S. Meng and H. Tian, *Sol. Energy Mater. Sol. Cells*, 2005, **88**, 23.
44 S. L. Li, K. J. Jiang, K. F. Shao and L. M. Yang, *Chem. Commun.*, 2006, 2792.
45 A. Hagfeldt and M. Gratzel, *Chem. Rev.*, 1995, **95**, 49.
46 K. Hara, M. Kurashige, Y. Dan-oh, C. Kasada, A. Shinpo, S. Suga, K. Sayama and H. Arakawa, *New J. Chem.*, 2003, **27**, 783.
47 M. Nilsing, P. Persson and L. Ojamae, *Chem. Phys. Lett.*, 2005, **415**, 375.
48 M. Guo, R. He, Y. Dai, W. Shen, M. Li, C. Zhu and S. H. Lin, *J. Phys. Chem. C*, 2012, **116**, 9166.

49 K. Hara, T. Sato, R. Katoh, A. Furube, T. Yoshihara, M. Murai, M. Kurashige, S. Ito, A. Shinpo, S. Suga and H. Arakawa, *Adv. Funct. Mater.*, 2005, **15**, 246.
50 Q. Wang, W. M. Campbell, E. E. Bonfanatani, K. W. Jolley, D. L. Officer, P. J. Walsh, K. Gordon, R. H. Baker, M. K. Nazeeruddin and M. Gratzel, *J. Phys. Chem. B*, 2005, **109**, 15397.
51 S. Jungsuttiwong, T. Yakhanthip, S. Jungsuttiwong, T. Yakhanthip, Y. Surakhot, J. Khunchalee, T. Sudyoadsuk, V. Promarak, N. Kungwan and S. Namuangruket, *J. Comput. Chem.*, 2012, **33**, 1517.
52 L. Han, N. Koide, Y. Chiba, A. Islam, R. Komiya, N. Fuke, A. Fukui and R. Yamanaka, *Appl. Phys. Lett.*, 2005, **86**, 213501.
53 J. Tomasi, B. Mennucci and R. Cammi, *Chem. Rev.*, 2005, **105**, 2999.
54 J. P. Perdew, K. Burke and M. Ernzerhof, *Phys. Rev. Lett.*, 1996, 77, 3865.
55 A. Schaefer, C. Huber and R. Ahlrichs, *J. Chem. Phys.*, 1994, **100**, 5829.
56 N. M. O'Boyle, A. L. Tenderholt and K. M. Langner, *J. Comput. Chem.*, 2008, **29**, 839.
57 M. J. Frisch, G. W. Trucks, H. B. Schlegel, G. E. Scuseria, M. A. Robb, J. R. Cheeseman, G. Scalmani, V. Barone, B. Mennucci, G. A. Petersson, H. Nakatsuji, M. Caricato, X. Li,; H. P. Hratchian, A. F. Izmaylov, J. Bloino, G. Zheng, J. L. Sonnenberg, M. Hada, M. Ehara, K. Toyota, R. Fukuda, J. Hasegawa, M. Ishida, T. Nakajima, Y. Honda, O. Kitao, H. Nakai, T. Vreven, J. A. Montgomery Jr, J. E. Peralta, F. Ogliaro, M. Bearpark,; J. J. Heyd, E. Brothers, K. N. Kudin, V. N. Staroverov, R. Kobayashi, J. Normand, K. Raghavachari, A. Rendell, J. C. Burant, S. S. Iyengar, J. Tomasi, M. Cossi, N. Rega, N. J. Millam, M. Klene, J. E. Knox, J. B. Cross, V. Bakken, C. Adamo, J. Jaramillo, R. Gomperts, R. E. Stratmann, O. Yazyev, A. J. Austin, R. Cammi, C. Pomelli, J. W. Ochterski, R. L. Martin, K. Morokuma, V. G. Zakrzewski, G. A. Voth, P. Salvador, J. J. Dannenberg, S. Dapprich, A. D. Daniels, O. Farkas, J. B. Foresman, J. V. Ortiz, J. Cioslowski and D. J. Fox, *Gaussian 09, Revision B.01*, Gaussian, Inc., Wallingford CT, 2010.
58 D. H. Bhaskar and H. D. Rajesh, *Tetrahedron Lett.*, 1996, **37**, 6375.